

**A STUDY OF STRUCTURE AND DYNAMICS OF
PROCHIRAL N-C AXIS FOR ASYMMETRIC TRANSITION
METAL CATALYSIS, WITH PHOSPHOROUS-31 (V) BY 3D NMR
SPECTROSCOPY COMBINED WITH MO CALCULATION**

**Yohko Sakamoto,^{*1} Kazuhiro Kondo,² Maiko Tokunaga,¹ Kumiko Kazuta,²
Hiroko Fujita,¹ Yasuoki Murakami¹, and Toyohiko Aoyama²**

¹School of Pharmaceutical Sciences, Toho University, Miyama 2-2-1,
Funabashi, Chiba 274-8510, Japan ² Faculty of Pharmaceutical Sciences,
Nagoya City University, Tanabe-dori, Mizuho, Nagoya 467-8603

*Corresponding author. Tel: +81 47 472 1282

E-mail: sakamoto@phar.toho-u.ac.jp.

Abstract – We have synthesized five kinds of prochiral N-C axis for asymmetric transition metal catalysis with phosphorus-31 (V) and investigated their mobility in solution by measuring ³¹P NMR spin-lattice relaxation time (T₁). 1-(S)-N-[2-(diphenylphosphinyl)naphthyl-2-(hydroxymethyl)pyrrolidine; compound (**1b**), and 1-(S)-N-[2-(diphenylphosphinyl)naphthyl]-2-(pyrrolidinylmethyl pyrrolidine; compound (**1e**) was assigned on the basis of NMR spectral data. From the vicinal ³¹P ¹H and ¹H ¹³C coupling constants of J resolution spectra on the 3D NMR spectra, the dihedral angles of compounds (**1b**), and (**1e**) were determined. The optimum stable structures of these compounds were obtained on the basis of NMR spectral data combined with molecular orbital calculations.

New approaches to ligand design for asymmetric catalysis have been investigated extensively.¹ Conformational analysis of that naked ligand is sometimes useful in deducing the conformation of a catalyst. However, the detailed structure and the dynamics of the Pro N-C axial chirality with phosphorus-31 (V) in solution remained to be studied. Accordingly, we synthesized compounds (**1a**)-(**1e**) and studied their conformation and mobility by NMR spectroscopy. We found that the dihedral angles, indicated by the thick line in Figure 1, of compounds (**1b**) and (**1e**) are not relevant to the whole conformation of the ligand. First, we report that the complete assignments of the NMR chemical shifts for these two test compounds (**1b**) and (**1e**) were achieved by additional standard methods (DQFCOSY, phase sensitive NOESY, and HOHAHA) combining the DPGSE HMQC,

DPFGSE-HMQC-TOCSY and HMBC spectra. Next, we describe the conformation of compounds (**1b**) and (**1e**) was determined on the basis of ^1H , ^{13}C and ^{31}P coupling constants by 3D NMR spectra. Hetero-nuclear long-range coupling constants are important for the structural elucidation and conformational analysis of organic and biomolecular compounds. Vicinal coupling constants can be correlated with dihedral angles in the Karplus relationship.^{2,3} The dihedral angles corresponding to $^3J_{\text{H-P}}$ and $^3J_{\text{H-C}}$ are calculated by means of the Karplus equations which take into account the dependency on the substitution pattern from Pro N-C axial chirality with phosphorus-31 (V). Moreover, the dynamic phenomena affecting the dihedral angles of compounds (**1a**) ~ (**1e**) were demonstrated by the phosphorus-31 (V) NMR spin lattice relaxation data and theoretical analysis. The backbone dihedral angles of $^3J_{\text{H3-P}}$, $^3J_{\text{H12-P}}$, $^3J_{\text{H16-P}}$, $^3J_{\text{H18-P}}$ and $^3J_{\text{H22-P}}$ can be estimated from $^3J_{\text{H-P}}$ coupling constants between phosphorus and its substituents. The values of ^{31}P T1 were used to determine the local mobility of the molecules. This may reflect the mobility around the $^3J_{\text{H-P}}$ coupling constant.

RESULTS AND DISCUSSION

COMPLETE ASSIGNMENTS OF THE NMR CHEMICAL SHIFTS

Since the assignments of the ^{13}C NMR signals for these compounds have not been reported, we analyzed their 2D NMR spectra, mainly HMQC-TOCSY, HMBC spectra in detail. We assigned all the ^1H and ^{13}C NMR chemical shifts of compounds (**1b**) and (**1e**). Since the two compounds are different in the bulkiness of the substitution groups (X), the assignments are useful in discussing their mobility. The structural numbering scheme and the sign of dihedral angles for the compounds are presented in Figure 1 and the pertinent ^1H and ^{13}C chemical shifts are summarized in Tables 1 and 2 for compounds (**1b**) and (**1e**). ^1H observed FG (Field gradient) phase-sensitive two-dimensional NOESY, HOHAHA spectra were used for the NMR spectral measurements. 2D NOESY experiments were performed to establish the spatial orientations. The NOE cross peaks were observed between H8 (7.97 ppm) and H23 (3.05 ppm) and H26 (3.96 ppm) and H25 (2.16 ppm) for compound (**1b**) and between H8 (8.05 ppm) and H25 and H26 (2.23, 1.81 ppm) and H27 (2.33 ppm) for compound (**1e**). These findings are consistent with the signals of the FG-DQFCOSY, and FG-HOHAHA spectra. Next, we take advantage of combining DPGSE HMQC, TOCSY and the HMBC spectra for compounds (**1b**) and (**1e**).^{2~4} Two-dimensional ^1H observed DPGSE HMQC spectra of compounds (**1b**) and (**1e**) permitted distinction between ^1H and ^{13}C by restricting the observed frequency range. DPGSE-HMQC-TOCSY and HMBC spectra of compounds (**1b**) lead to significantly better results as shown in Figure 2 and 3. On the $^2J_{\text{H-C}}$ of

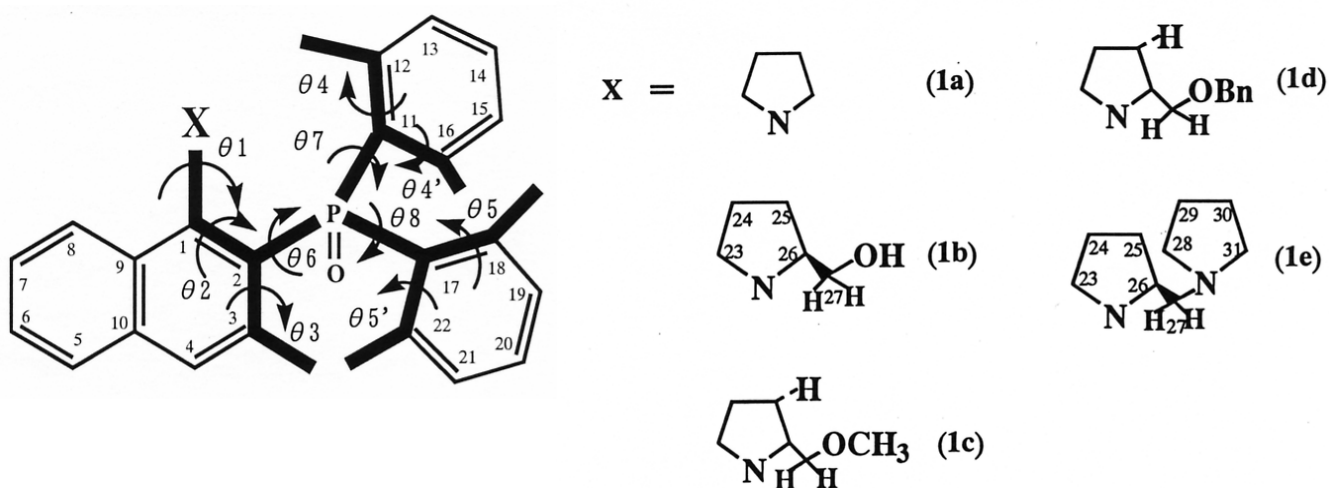


Figure 1. Compounds (1a)-(1e)

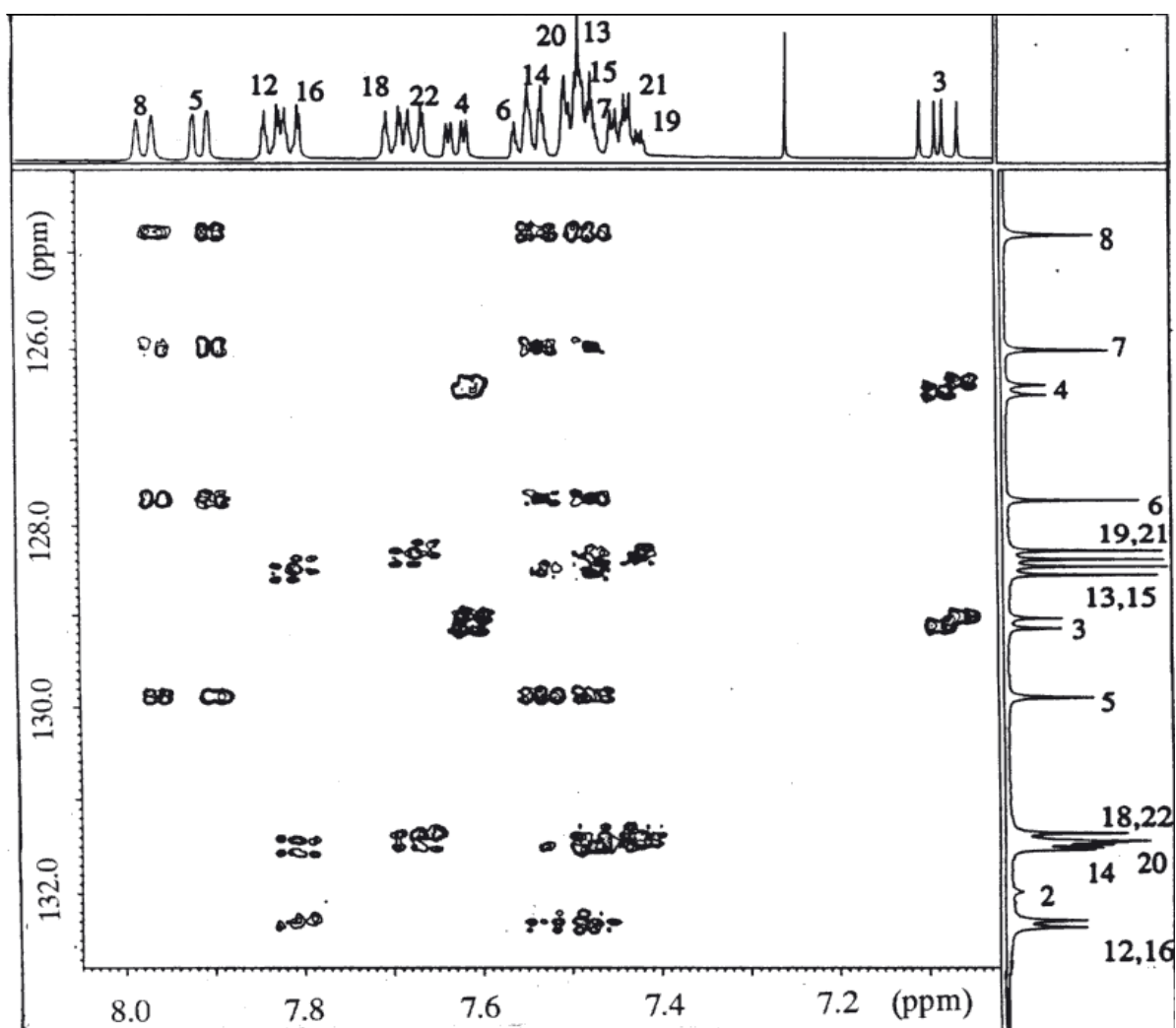


Figure 2. ^1H observed 2D ^1H - ^{13}C HMQC-TOCSY spectra of compound (1b); the observation frequency range was restricted.

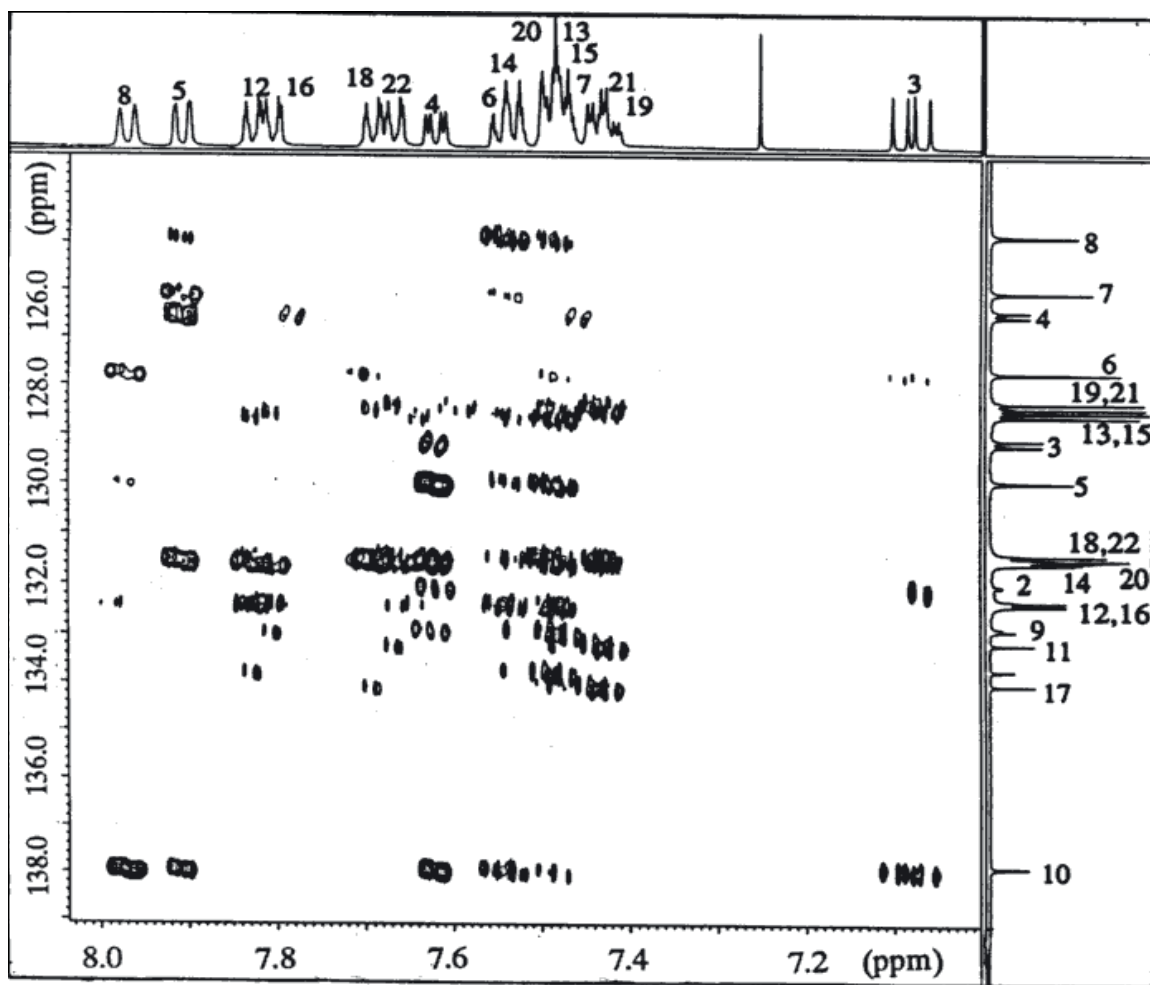


Figure 3 ¹H observed 2D ¹H-¹³C HMBC spectra of compound (**1b**); the observation frequency range was restricted.

compound (**1b**), there are correlations of C12, C14, C16 with H13 and H15; C20 with H19; C18, C22 with H19, H21; C5 with H6; C3 with H4; C13 and C15 with H12, H14, H16; C19, C21 with H18, H22; C6 with H5, H7; C4 with H3; C7 with H6, H8; C8 with H7. The FG-HMBC experiment confirms the H-C bond *via* the long-range correlations $^2J_{\text{H-C-C}}$ and $^3J_{\text{H-C-C-C}}$. In particular, quaternary carbon atoms (C1, C2, C9, C10, C11, and C1 (**1b**), there are correlations of C10 with H4 and H5; C12, C14, C16 with H13 and H15; C2 with H3; C18, C20, C22 with H19, H21; C5 with H4; C3 with H4; C13 and C15 with H12, H16; C19, C21 with H18, H21; C7 with H6; C8 with H7; C26 with H25, H27; C23 with H24; C25 with H24; and C24 with H25. On the $^3J_{\text{H-C-C-C}}$ of compound (**1b**), there are correlations of C1 with H3 and H8; C10 with H3 and H6; C17 with H19 and H21; C11 with H13 and H15; with H4 and H7; C12 and C16 with H14; C2 with H4; C14 with H12 and H16; C18, C20 and C22 with H18 and H22; C5 with H7; C13 and C15 with H13 and H15; C19 and C21 with H19 and H21; C6 with H8; C4 with H5; C7 with H5;

C8 with H6; C26 with H24; C27 with H25; C23 with H25; C25 with H27. These results for compound (**1b**) are summarized in Table 1 and those for compound (**1e**) in Table 2. We could obtained the dihedral angles of H3-C2-C3-P (θ 3), C1-C2-C3-H3 (θ 3), H12-C12-C11-P (θ 4), H16-C16-C11-P (θ 4'), H18-C18-C17-P (θ 5) and H22-C22-C17-P (θ 5') by these detailed assignments of ^1H and ^{13}C NMR spectrum. For the compound (**1e**), the spectrum was assigned by several kinds of NMR methods in the same way as described for compound (**1b**).

Table 1 ^1H and ^{13}C Chemical shifts for compound (**1b**) at 40°C in CDCl_3

	δC	HMQC	HMBC	
		δH	$^2\text{J}(\text{H,C})$	$^3\text{J}(\text{H,C})$
C-1	153.57			H-3, H-8
C-10	137.87		H-4, H-5	H-3, H-6
C-17	134.03			H-19, H-21
C-11	133.17			H-13, H-15
C-9	132.89			H-4, H-7
C-12, 16	132.32	7.830, 7.810	H-13, H-15	H-14
C-2	132.01		H-3	H-4
C-14	131.52	7.530	H-13, H-15	H-12, H-16
C-20	131.46	7.481	H-19, H-21	H-18, H-22
C-18, 22	131.41	7.690, 7.670	H-19, H-21	H-18, H-22
C-5	129.90	7.910	H-4	H-7
C-3	129.10	7.090	H-4	
C-13, 15	128.52	7.480, 7.479	H-12, H-16	H-13, H-15
C-19, 21	128.34	7.425, 7.435	H-18, H-21	H-19, H-21
C-6	127.69	7.540		H-8
C-4	126.44	7.620		H-5
C-7	125.99	7.478	H-6	H-5
C-8	124.82	7.970	H-7	H-6
C-26	67.82	3.960	H-25, H-27	H-24
C-27	63.36	3.350, 3.610		H-25
C-23	55.15	3.050, 1.920	H-24	H-25
C-25	28.22	2.160, 2.160	H-24	H-27
C-24	26.82	1.810, 1.810	H-25	

Table 2 ^1H and ^{13}C Chemical shifts for compound (**1e**) at 40°C in CDCl_3

	δC	HMBC		
		δH	$^2\text{J}(\text{H,C})$	$^3\text{J}(\text{H,C})$
C-1	152.08			H-3, H-8
C-10	136.98		H-4, H-5	H-3, H-6, H-8
C-11	134.63			H-13, H-15
C-17	134.11			H-19, H-21
C-12, 16	131.84	7.782, 7.758	H-13, H-15	H-12, H-14, H-16
C-18, 22	131.62	7.706, 7.683	H-19, H-21	
C-14	131.33	7.490	H-13, H-15	H-12, H-16
C-20	131.30	7.485		H-18, H-22
C-3	129.51	7.179		
C-2	129.04		H-3	H-4
C-5	129.03	7.846		H-4
C-13, 15	128.38	7.442, 7.435	H-14	H-13, H-15
C-19, 21	128.35	7.410, 7.418	H-20	H-19, H-21
C-9	128.23			H-4, H-7
C-6	127.82	7.530		H-8
C-7	126.26	7.480		H-5
C-4	125.48	7.572	H-3	H-5
C-8	125.31	8.053	H-7	H-6
C-26	62.75	4.269	H-25	H-24
C-23	54.23	2.907, 2.907	H-24	H-25
C-24	54.13	1.664, 1.778	H-25	
C-31	54.08	2.265, 2.265	H-24	
C-25	31.30	2.226, 1.812	H-24	H-23
C-28	24.64	2.226, 1.812	H-29	H-25
C-29, 30	23.29	1.520	H-31	H-31
C-27	21.43	2.330, 2.330	H-26	H-25

MOST STABLE CONFORMATION

A gradient-selected J-HMBC experiment is also an excellent 3D NMR method for estimating hetero-nuclear long-range $^3\text{J}_{\text{HP}}$ and $^3\text{J}_{\text{HC}}$ coupling constants in organic phosphates such as compounds (**1b**) and (**1e**) having phosphorus-31 (V) in the chiral ligand. Conformation of prochiral N-C axis,

Table 3 Coupling constants

	Compound (1b)	Compound (1e)
(Hz)		
$^3J_{\text{H3-P}}$	10.09	12.20
$^3J_{\text{H12-P}}$	10.80	11.60
$^3J_{\text{H16-P}}$	11.50	11.60
$^3J_{\text{H18-P}}$	10.65	10.45
$^3J_{\text{H22-P}}$	11.00	11.50
$^3J_{\text{C1-H3}}$	8.80	6.40

Table 4 Dihedral angles of compound (1b)

	Dihedral angles	From NMR data (CDCl ₃)	From MO calculations
A	OH-C27-C26-N N-C27-C26-N H27-C27-C26-N		-80.16 43.36
B	C27-C26-N-C1		-0.74
1	O26-N-C1-C2		-102.08
2	N-C1-C2-C3 N-C1-C2-P		-179.75 0.26
3	C1-C2-C3-H3 H3-C2-C3-P	160.60, 19.20 139.70, 11.70	
4	H12-C12-C11-P	142.00	
4'	H16-C16-C11-P	143.00	
5	H18-C18-C17-P	141.60, 00	
5'	H22-C22-C17-P	142.70	
6	C3-C2-P-C11		173.57
7	C2-P-C11-C12 C2-P-C11-C16		-77.37 106.50
8	C2-P-C17-C22 C2-P-C11-C18		146.88 14.51

(S)-*N*-[2-(diphenylphosphino)naphthyl]-2-(pyrrolidinylmethyl)pyrrolidine for asymmetric transition metal catalysis with phosphorus-31 (V) is primarily characterized by the torsion angles of compound (**1**). The main dihedral angles (marked with θ in Table 4) were determined by 3DNMR in CDCl₃ solution. For the dihedral angles O26-N-C1-C2 (θ_1), N-C1-C2-C3, N-C1-C2-P (θ_2), C3-C2-P-C11 (θ_6), C2-P-C11-C12, C2-P-C11-C16 (θ_7) and C2-P-C17-C22 (θ_8), OH-C27-C26-N (θ_A), N-C27-C26-N (θ_A), H27-C27-C26-N (θ_A), and C27-C26-N-C1 (θ_B) could not be determined by J resolution spectra on the 3D NMR spectra, and the results of MO calculations were used. We noted the dihedral angles H3-C2-C3-P (θ_3), C1-C2-C3-H3 (θ_3), H12-C12-C11-P (θ_4), H16-C16-C11-P (θ_4'), H18-C18-C17-P (θ_5) and H22-C22-C17-P (θ_5') differ according to the substitution pattern. The influence of the substitution pattern upon proton-phosphorus 31 coupling shows that the bulkiness of the substitution groups (X) is important. This is probably due to the absence of the nearest neighbors, which causes the internal rotation to slow and the ³¹P to relax slowly. The dihedral angles, which are needed to determine the optimum conformation, can be obtained by substituting the experimental values of the ³J_{HP} and ³J_{H-C} coupling constants into eqs. (1) and (2). We used the method of J resolution spectrum on 3D NMR to obtain the main dihedral angles. The short- and long-range coupling constants, such as ³J_{HP}, ⁴J_{HP}, ⁵J_{HP}, ⁶J_{HP}, and ⁷J_{HP}, were obtained for compounds (**1b**) and (**1e**); we used the ³J_{HP} coupling constants for the present purpose. The values of vicinal coupling constants of ³J_{H3-P}, ³J_{H12-P}, ³J_{H16-P}, ³J_{H18-P}, and ³J_{H22-P} of compounds (**1b**) were 10.09, 10.80, 11.50, 10.65, and 11.0 Hz, respectively, as shown in Figure 4. By fitting a sine curve to the experimental data by the method of 3D J-resolved HMBC experiments, accurate ⁿJ × coupling constants are obtained. The signal amplitude of spectra with increasing coupling evolution time shows the characteristic sin (× J_{PH} ×) dependence. Vicinal coupling constants can be correlated with dihedral angles in the Karplus relationship (1) and (2),^{2,3} of the following type.

$${}^3J(\text{HP}) = 15.3 \cos 2\theta - 6.1 \cos \theta + 1.6 \quad (1)$$

$${}^3J(\text{CH}) = 4.26 - 1.00 \cos \theta + 3.456 \cos 2\theta \quad (2)$$

The Karplus dihedral angle relationship has been the effective tool in conformational analysis by NMR. In order to derive reliable Karplus parameterization, it is desirable to have at least one calibration point in the 0°- 60° range. The long-range evolution delay is varied by shifting a 180° pulse in the constant time delay max. The vicinal coupling constants of ³J_{H3-P}, ³J_{H12-P}, ³J_{H16-P}, ³J_{H18-P}, ³J_{H22-P}, and ³J_{C1-H3} of compounds (**1b**) and (**1e**) were obtained in CDCl₃ by 3D NMR measurements as listed in

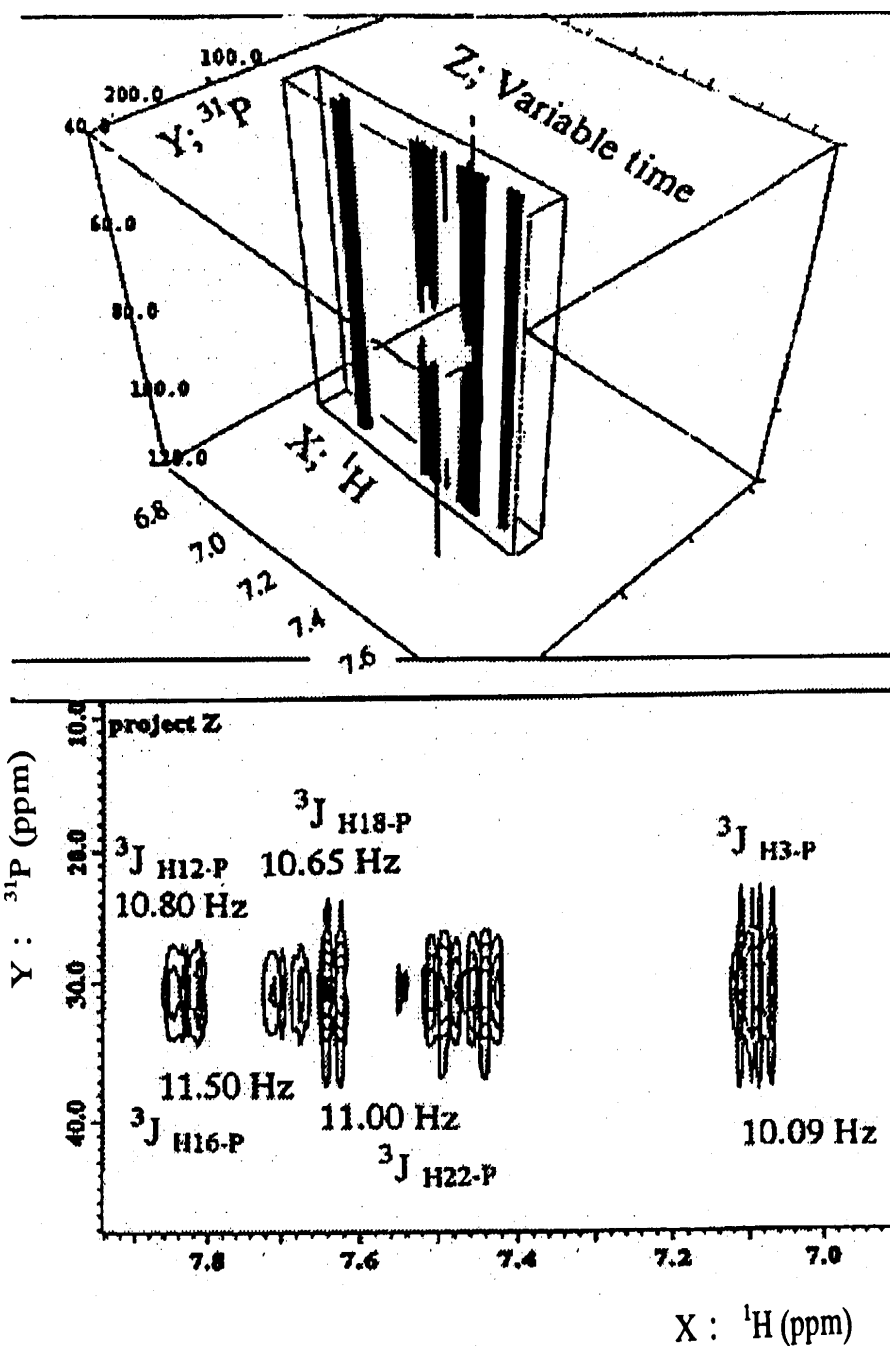


Figure 4. The 3D NMR spectrum of compound (**1b**)

Table 3. The dihedral angle for H3-C2-C3-P (θ_3) of compound (**1b**) is determined from the experimental value of ${}^3J_{\text{H3-P}}$, 10.09 Hz. Substituting to this value into eqs. (1), we obtained two values of the angle, 139.7° and 11.7° . The two values were investigated from the point of view of stability and the value of 139.7° was chosen as the most appropriate value for θ_3 . Similarly, the dihedral angles for H12-C12-C11-P (θ_4), H16-C16-C11-P (θ_4'), H18-C18-C17-P (θ_5), H22-C22-C17-P (θ_5') and H3-C2-C3-P (θ_3) could be determined by using the experimental values of ${}^3J_{\text{H12-P}}$, ${}^3J_{\text{H16-P}}$, ${}^3J_{\text{H18-P}}$, ${}^3J_{\text{H22-P}}$,

and $^3J_{\text{C1-H3}}$, respectively. The results for compounds **(1b)** and **(1e)** are shown in Tables 4 and 5. From these data, we can deduce the conformations of compounds **(1b)** and **(1e)** in CDCl_3 as shown in Figure. 5. These conformations were energetically most stable in CDCl_3 .

Table 5 Dihedral angles of compound (1e)

	Dihedral angles	From NMR data (CDCl_3)	From MO calculations
A	OH-C27-C26-N		
	N-C27-C26-N		161.06
	H27-C27-C26-N		38.58
B	C27-C26-N-C1		-179.65
	O26-N-C1-C2		-108.86
1	N-C1-C2-C3		7.76
	N-C1-C2-P		-1.67
3	C1-C2-C3-H3	145.60	
	H3-C2-C3-P	149.80, 47.20	
4	H12-C12-C11-P	144.60	
4'	H16-C16-C11-P	144.60	
5	H18-C18-C17-P	140.00, 10.80	
5'	H22-C22-C17-P	143.00	
6	C3-C2-P-C11		118.51
7	C2-P-C11-C12		28.13
	C2-P-C11-C16		100.06
8	C2-P-C17-C22		142.52
	C2-P-C11-C18		40.58

Table 6 ^{31}P Chemical shifts and T1 values for compounds (1a)-(1e) at 40°C in CDCl_3

Compound	P	^{31}P T1 (sec)
(1a)	29.4909	3.77
(1b)	27.5599	3.00
(1c)	35.9088	2.06
(1d)	32.2139	1.80
(1e)	30.0624	1.70

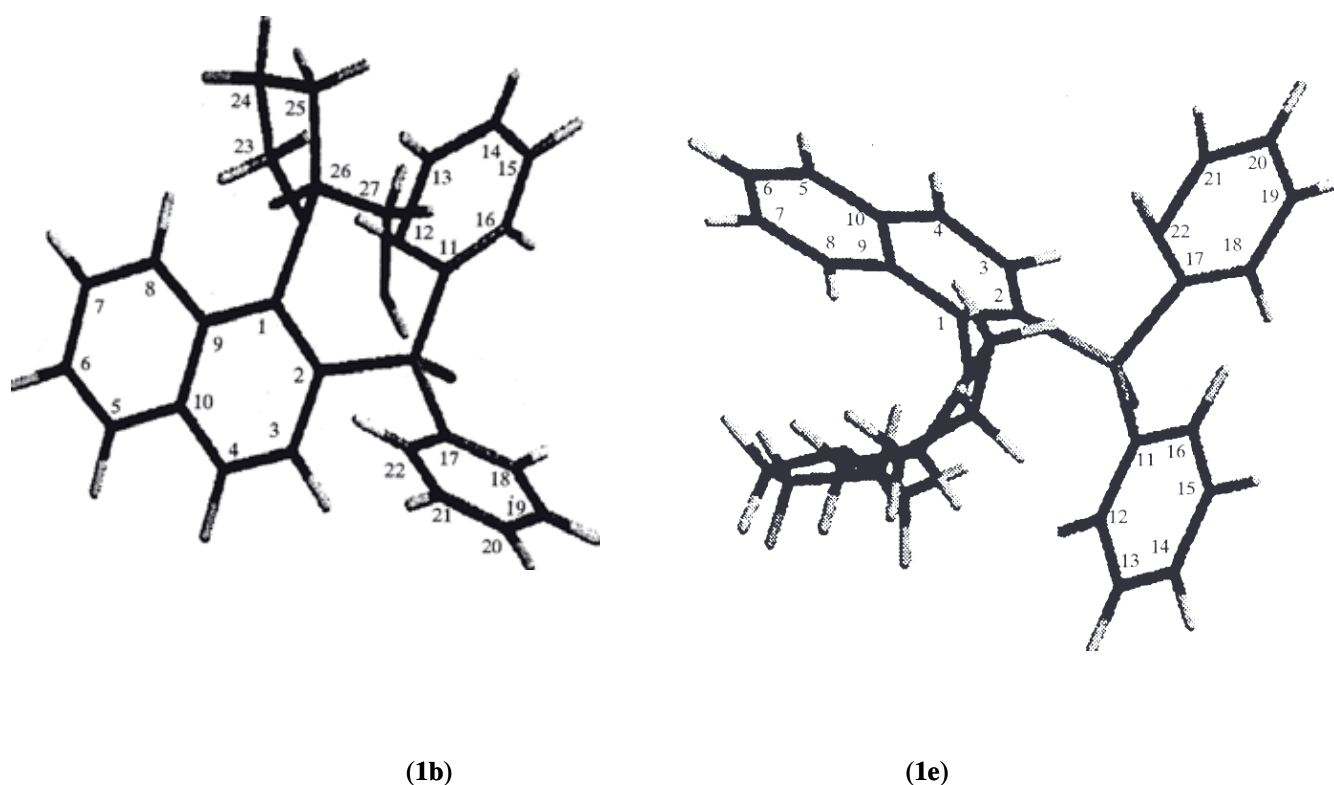


Figure 5. Most stable conformation of compounds (**1b**; left) and (**1e**; right)

MOLECULAR DINAMICS

It is necessary to analyze T1 of compound (**1**), because the direction of lone pair for nitrogen of the substitution groups (X) is enormously influenced by the T1 value. To check the influence of the type of bonding on the $^3J_{\text{H-P}}$, we selected five compounds (**1a**) ~ (**1e**) and the phosphorus-31(V) T1 were measured. The spin-lattice relaxation time ($^3\text{PT1}$) of the phosphorus NMR signals is widely used to determine the local mobility of molecules. These results are listed in Table 6. As shown in Table 6, the experimental ^3P T1 values of compounds (**1a**) ~ (**1e**) were 3.77, 3.0, 2.06, 1.80, and 1.70 sec, respectively. Judging from the influence of the substitution fragments, it is expected that the T1 values of compound (**1**) vary systematically in turn of compound (**1a**) > (**1b**) > (**1c**) > (**1d**) > (**1e**). From this $^3\text{PT1}$ dependence for the molecular dynamics, we estimated the mobility of the five phosphorus-31 (V) compounds, which differ in the substitution groups (X) for Pro N-C axial chirality. The bulkier the substitution group (X) becomes, the shorter ^3P T1 becomes. It should be noted that the ^3P T1 value of compound (**1b**) is smaller than that of compound (**1e**) by 1.3s. Since compound (**1e**) has more volume than compound (**1b**), the bulkiness of the latter seems to be smaller in CDCl_3 than that of the former from

the point of view of molecular dynamics. The longest ^{31}P T1 values are observed for compound (1a). For an example compound (1a) indicates a naphthalene ring and the lone pair of the hetero atoms are located parallel to each other, the T1 value becomes much smaller. Furthermore, for an example compounds (1a) ~ (1e) which have much bigger side chain, the plane of the naphthalene ring and the lone pair of a heteroatom is twisted progressively greater and their T1 values become much bigger. The influence of the substitution pattern upon proton-phosphorus 31 coupling shows that the bulkiness of the substitution groups (X) is important. This is probably due to the absence of the nearest neighbors, which causes the internal rotation to be slow and the ^{31}P to relax slowly.

CONCLUSION

Complete NMR assignments of compounds (1b) and (1e) were made by combining the results of phase-sensitive 2D NOESY, HOHAHA, DPGSE-HMQC, DPGSE HMQC-TOCSY, and phase-sensitive FG-HMBC methods. The present paper demonstrates that the coupling constants of ^{31}P - ^1H measurements provide a new insight into phosphitylated structures and give information complementary to that obtained from other NMR methods. Prochiral N-C axis, (S)-N-[2-((diphenylphosphino)naphthyl)-2-(pyrrolidinylmethyl)pyrrolidine for asymmetric transition metal catalysis with phosphorus-31 (V) has opened a new avenue to conformational analysis using $^3J_{\text{HP}}$ coupling constants, in addition to $^3J_{\text{CH}}$, which define the torsion angles. Phosphorus nuclear magnetic resonance (NMR) is playing a role in structural characterization and qualitative identification of different phosphorus compounds. Using the bond angles and bond lengths obtained from NMR spectrum and molecular orbital studies, we were enabled to postulate the favored spatial orientation of the functional groups of compounds (1b) and (1e) in solution. In particular, spin-spin coupling constants are useful in determine the composition of X and the positions and configuration for compound (1) by using the 3D NMR combined with molecular orbital method.

EXPERIMENTAL

^1H , ^{13}C and ^{31}P NMR spectra were measured on a JEOL ECP-500 NMR spectrometer and were recorded in δ units, parts per million (ppm). Experiments were performed on five phosphorus derivatives of phosphorus-31 (V) on the chiral ligand. Compounds (1a) to (1e) were synthesized by the method previously reported.¹ Among these compounds, compounds (1b) and (1e) were studied by NMR spectroscopy. In order to reduce the spin lattice relaxation times, we used $180^\circ\text{-}\tau\text{-}90^\circ$ (T1) inversion recovery method for ^{31}P . For phase-sensitive NOESY spectra, we used the same ^1H spectral windows

and f2 data points with 256 increments linearly predicted to 1024 with a mixing time of 0.85s and a relaxation delay of 1.0 s. The double pulsed-filled-gradient-spin-echo (DPFGSE) sequence was used for the excitation sculpting techniques.²⁻⁴ The BIRD (Bilinear Rotation Decoupling) method can be used in this DPGFSE pulse sequence. Its effect is to selectively invert protons attached to carbon-12 while leaving intact protons bound to carbon-13 nuclei. For the DPGFSE experiments a recycle delay of 2s was employed, operating at 500 MHz at 40° C by using a deuterium lock system. Filled rectangles are 90° pulses; open rectangles are 180° pulses that were conventional 180° pulses on the proton channel and composite 90°x, 240°y, 90°x inversion pulses on the ¹³C channel. The bird elements are labeled by the phase of the central proton 180° pulse. CDCl₃ was used as solvent. All PFGs were 1 ms and followed by a recovery delay of 200 μs. The concentration of the sample was 0.0731 mol/l. The chemical shifts were measured relative to tetramethylsilane. ¹H observed FG (Field Gradient) Double Quantum filtered correlated spectroscopy (FG-DQFCOSY) was used for measurement of absolute values and phase-sensitive two-dimensional FG-NOESY and FG-HOHAHA spectra. For 3D NMR experiment an X axis (F1; ³¹P), Y axis (F2; ¹H), Z axis (F3; variable time) data matrix was acquired with τ max = 120 ms resulting in a 16 h measuring time. Ab initio molecular orbital calculations were performed with the software package SPARTAN. Pro V 1.08, and optimum conformations of compounds (**1b**) and (**1e**) were obtained, using the 6-31G-basis set for the calculations.

REFERENCES

1. K. Kondo, K. Kazuta, H. Fujita, Y. Sakamoto, and Y. Murakami, *Tetrahedron*, 2002, **58**, 5209.
2. P. P. Lankhorst, C. A. Haasnoot, C. Er Kelens, and C. Altona, *J. of Biomolecular Structure and Dynamics*, 1984, **1**, 1387 JHCOP, 15, 3.
3. J. L. Marshall (ed), '*Carbon-Carbon and Carbon-Proton NMR Couplings*,' Verlag, Chemie International, Deerfield Beach, Fa, 1983, p22.
4. T. L. Hwang and A. J. Shaka, *J. Magn. Reson.*, 1995, **A 112**, 275.
5. C. Emetarom, T. L. Hwang, G. Marckin, and A. J. Shaka, *J. Magn. Reson.*, 1995, **A 115**, 137.
6. G. Mackin and A. J. Shaka, *J. Magn. Reson.*, 1996, **A 118**, 247.